Advanced Industrial and Engineering Polymer Research 2 (2019) 1–12

Contents lists available at ScienceDirect

Advanced Industrial and Engineering Polymer Research

journal homepage: http://www.keaipublishing.com/aiepr

# Processing and strain induced crystallization and reinforcement under strain of poly(1,4-*cis*-isoprene) from Ziegler–Natta catalysis, *hevea brasiliensis*, *taraxacum kok-saghyz* and *partenium argentatum*

Sara Musto [a, 1], Vincenzina Barbera [a], Gaetano Guerra [b], Maurizio Galimberti [a, *]

[a] Politecnico di Milano, Department of Chemistry, Materials and Chemical Engineering G. Natta, Via Mancinelli 7, 20131, Milano, Italy
[b] Universita` di Salerno, Department of Chemistry and Biology, Via Giovanni Paolo II 132, 84084, Fisciano, SA, Italy

ARTICLE INFO

*Article history:*
Received 15 June 2018
Accepted 6 August 2018

*Keywords:*
Strain induced crystallization and reinforcement
poly(isoprene)s
Hevea brasiliensis
*taraxacum kok-saghyz*
*partenium argentatum*

ABSTRACT

Strain induced crystallization and reinforcement were studied for poly(isoprene)s from the following sources: Ziegler–Natta catalysis, *hevea brasiliensis* (HNR), *taraxacum kok-saghyz* (TKS), known as the russian dandelion, *partenium argentatum* (GR), known as guayule. Two HNR samples were studied, with high (HNR-H) and low (HNR-L) molar mass. Investigated guayule samples were: as isolated from the latex (GR-R) and after extraction with acetone (GR-P). All of the samples had weight average molar mass higher than $1.5 \times 10^6$ Da. TKS was found to be the most stereoregular sample, with undetectable amounts of stereoerrors. Wide angle X-Ray diffraction patterns were collected on samples, unstretched after processing and during stretching, up to 5 as the strain ratio. Quasi-static tensile measurements were performed. HNR and GR-P exhibited rubber crystallinity already in the undeformed state and the orientation of their crystalline phase remained low also for the highest strain ratios. GR-R and TKS were amorphous at low strain and developed highly oriented crystalline phases under stretching. TKS developed extraordinary mechanical reinforcement under stretching: stresses at large elongations were much higher than those obtained with HNR. It is thus shown that the formation of highly oriented crystalline phases brings large mechanical reinforcement.

In conclusion, an amorphous NR sample from a natural source, such as TKS, which has high molar mass and does not contain non rubber components which could act as plastifiers, is able, under stretching, to develop crystallinity and a high degree of axial orientation. Crystallization occurs at high strain ratio, when the chains are prevailingly aligned. The biosynthesis of TKS is likely to play a strategic role, as it promotes the chain end crosslinking of the polymer chains.



## 1. Introduction

Natural rubber (NR) is poly(1,4-cis-isoprene), a polymer with very high stereoregularity [1–4]. It is the most important rubber: world-wide consumption is more than 12 million tonn/year and is steadily increasing [5]. History of natural rubber is fascinating [6], from the first examples of processing, use and transport in Mesoamerica, 1600 years B.C. [7,8], to the discovery of vulcanization by Charles Goodyear [9]. Meso-americans were able to obtain elastic and wear resistant rubber, suitable to prepare rubber balls, sandal soles and rubber bands, mixing juice from *Ipomoea alba* (morning glory vines) with latex from *Castilla elastica* trees. Indeed, NR has unique properties: outstanding strength [10,11] and tack [12–14] in the uncured state and, upon crosslinking, very high tensile strength [15,16] and crack growth resistance, in fatigue [17–23] and in static [24–28] loading conditions. In particular, the crack growth resistance is a key property, which allows to use NR for airplane tyres, heavy truck and base isolators to limit and prevent damages due to seismic vibrations.

Large scale industrial application of natural rubber has been mostly based on NR from *Hevea Brasiliensis*, but more than 2000 species of plants produce poly(1,4-cis-isoprene) [4]. In the last decades, research on alternative sources of NR has been very active. In fact, major problems hang on NR from hevea brasiliensis (HNR) like the sword of Damocles [29]: diseases could lead to significant crop loss, plantations are concentrated in relatively small geografic areas and shortage can be predicted, due to increasing consumption. Preferred alternative sources of natural rubber are *taraxacum*

* Corresponding author.
*E-mail address:* maurizio.galimberti@polimi.it (M. Galimberti).
[1] Present address: Pirelli Tyre, Viale Piero e Alberto Pirelli 25, 20126 Milano (I).

https://doi.org/10.1016/j.aiepr.2018.08.003

*kok-saghyz*, known as the russian dandelion and *partenium argentatum*, known as guayule. Papers are available since the beginning of the last century, on taraxacum [30,31] and on guayule [32–40]. Biosynthesis studies are performed, to improve the rubber productivity from alternative sources [41–46].

It is widely acknowledged that NR samples, from Hevea Brasiliensis and from other sources, do not contain only poly(isoprene) but also non rubber components, in different amount, depending on the source as well as on plantation and farming conditions. Careful studies have to be performed in order to assess the chemical composition of rubber samples [47,48], because, as discussed in the following, non rubber components have a strong effect on the properties of natural rubber, such as the strain induced crystallization (SIC) and the behavior in vulcanization.

SIC is the prompt development of crystallization under straining. Stretching NR over a threshold strain ratio triggers SIC, whose kinetics increases with the strain amplitude. It decreases as the temperature is raised and has not been observed at temperatures higher than 80 °C. Reviews on SIC of natural rubber are available [49–51]. Moreover, studies are reported on local strain response [52] segmental dynamics [53], mechanism of deformation [54], orientation and deformation mechanisms [55], morphology [56], kinetics [55,57,58] and time [59] of crystallization, crystallite structure [60,61], crystallite melting temperature [62], on the study of models [63,64], temperature dependence of mechanical properties [65], fatigue behaviour [66,67]. Explanation of the SIC phenomenon are based on the high stereoregularity of poly(isoprene) chains [2,3,68,69] and on the small melting entropy per statistical segment [70,71] More recently, the key role played by non rubber components has been elucidated [72–79]. It is acknowledged that polymer chain ends bear dimethylallyl groups modified with proteins and phospholipids with fatty acid ester groups. Branch-points by ionic and hydrogen bonds and via the formation of micelles are formed by poly(isoprene) chain ends. Linked and free saturated fatty acids have nucleating effect on NR crystallization. The effect of entanglements and endlinking networks [80,81], as well as of deproteinization [80] has been investigated. Studies on the cohesive strength [34] and on crystallizability under strain [35,37,38,40] have been reported for G-NR. Some of the authors have recently reported a comparative study of SIC for HNR and TKS [47].

It is known that poly(1,-cis-isoprene) from Hevea Brasiliensis promotes faster vulcanization than the synthetic homologue and this is attributed to the effect of non rubber components such as proteins.

Research here reported was focused on strain induced crystallization (SIC) and vulcanization of NR, comparing NR samples from *Hevea brasiliensis* (HNR), *taraxacum kok-saghyz* (TKS) and *parthenium argentatum* (GR) and a synthetic poly(1,4-cis-isoprene) sample (IR) from Ziegler–Natta catalysis. Two HNR samples were analyzed, with high (HNR-H) and low (HNR-L) molar mass. Chemical composition of HNR, G-NR and TKS samples was determined through thermogravimetric analysis (TGA), infrared (IR), $^{1}H$ and $^{13}C$ NMR spectroscopy. In particular, low molar mass components were isolated, through solvent extraction, and characterized. Wide Angle X-ray diffraction (WAXD) patterns were taken on samples stretched at different strain ratio ($\alpha$) and quasi-static measurements were performed, at room temperature.

## 2. Experimental part

### 2.1. Materials

Synthetic poly(1,4-*cis*-isoprene) (IR) (Nizhnekamskneftechim Export) had trade name SKI3.

Natural poly(1,4-*cis*-isoprene)s were as follows.

From *Hevea Brasiliensis*: STR20 from Eastern GR Thailandia – Chonburi (HNR-L), RSS3 from LTR L.T. Rubber Co Thailandia – Reyong (HNR-H).

From *partenium argentatum:* solid raw rubber (GR-R) was isolated (see below) from the latex obtained from Yulex Corporation. Purified rubber (GR-P) was obtained from GR-R, through extraction with ethyl acetate (see below).

From *taraxacum kok-saghyz*: solid rubber (TKS) was from NovaBioRubber Green Technologies Inc.

Acetone and ethyl acetate were from Aldrich (≥99%) and were used without purification.

2,2′-Dibenzamido diphenyl disulfide (DBD) (CAS Number: 135-57-9, chemical formula C26H20N2O2S2) was Renacit 11 from Lanxess.

### 2.2. Preparation of solid rubber samples

*Isolation of GR-R from rubber latex.* In a 15 cm diameter flat beaker were poured 30 mL of Guayule rubber latex, that formed a 2 mm thick continuous layer, dried for 48 h in a hood at room temperature in the absence of light. The quantity of GR-R obtained was 15 g.

*Preparation of GR-P.* GR - R (10 g) was finely sliced and placed into a brown laboratory glass bottle (DURAN ® GL 45) provided with a cap, and 500 mL of ethyl acetate were added. The suspension was left 24 h without stirring, in the absence of light. The solvent was poured off and the operation was repeated twice. The pure solid rubber was dried for 12 h at 30 °C, under nitrogen atmosphere. 8 g of pure rubber were eventually obtained.

*Extraction of non rubber components from poly(1,4-cis-isoprene) samples.* Samples were extracted with Soxhlet apparatus in refluxing acetone for 16 h, adopting the ISO1407 procedure.

*Reaction of TKS sample with $NaOCH_3$.* Reaction was carried out on 15 g of TKS sample, after extraction of non rubber components. Solid sample was first put in a 250 mL round bottomed flask, then dissolved in 100 mL of toluene, at 50 °C, under nitrogen. After dissolution, were added 400 mg of $NaOCH_3$ under nitrogen atmosphere. The reaction mixture was then maintained at 50 °C for 3 h. After cooling, 300 mL of methanol were added and the precipitated solid rubber was first removed and then dried at 30 °C under vacuum.

### 2.3. Preparation of HNR samples with different molar mass

50 g of poly(1,4-cis-isoprene) HNR-H were introduced into a Brabender type internal mixer and masticated at 100 °C for 1 min with rotors rotating at 60 rpm. 2,2′-Dibenzamido diphenyl disulfide was added in different amounts (0,05 and 0,1 phr) and mixing was performed for 4 min.

### 2.4. Characterization of poly(1,4-cis-isoprene) samples

*Determination of volatile components.* The amount of volatile components were determined by thermal gravimetric analysis (TGA), performed with a Mettler TGA SDTA/851 instrument in a flowing $N_2$ (flow rate 60 mL/min) from 30 °C to 300 °C with heating rate of 10 °C/min.

*Determination of fatty acids present in poly(1,4-cis-isoprene) samples.* Content and type of fatty acids were determined by GC-MS analysis. In a 100 mL conical flask equipped with a condenser were poured in sequence 2 g of solid rubber and 40 mL of a solution 4% (w/v) of $H_2SO_4$ in methanol. The reaction was carried out under reflux for 1 h. Upon cooling the suspension to room temperature, solid $NaHCO_3$ was added to achieve a neutral solution. Salts were removed by filtration, performed using a filter paper and a funnel. The liquid was brought to 100 mL by adding methanol into a

volumetric flask. 5 mL of such solution were put into a 30 mL test tube and mixed with 5 mL of heptane. The organic phase was washed, once, with 5 mL of brine. The upper phase was removed, dried on $Na_2SO_4$ and analyzed by GC-MS analysis.

*NMR analysis*. One-dimensional $^1H$ and $^{13}C$ NMR spectra were measured at 400 and 100 MHz, respectively, using a Bruker AV 400 equipped with a 5 mm multinuclear probe with reverse detection (Bruker, Rheinstetten, Germany). The solvent was deuterated Chloroform and the temperature was 27 °C. The experimental time for $^{13}C$ NMR spectra was typically 12 h (corresponding to more than 10,000 scans). Data were processed using TOPSPIN 1.1 or MestReNova.

*DSC analysis.* Calorimetric measurements were performed in a differential scanning calorimeter Mettler DSC 823e in a flowing $N_2$ atmosphere. The glass transition temperatures (Tg) were determined by DSC curves recorded at 10 °C/min.

*Preparation of samples for X-ray diffraction analysis under stretching* Samples were passed through a two roll mill for 5 times and pressed with 150 bar pressure in rectangular plates (thickness: 0.5 mm; width: 100 mm; overall length: 100 mm) at room temperature. Dumbbell were cut from the plates for the tensile tests.

*X-ray diffraction.* X-ray diffraction patterns were obtained at room temperature by a Philips X-ray generator (CuK$\alpha$ radiation) in transmission by using a cylindrical camera (radius = 57.3 mm) with the X-ray beam perpendicular to the sample surface. The WAXD patterns were recorded on a BAS-MS imaging plate (FUJIFILM) and processed with a digital imaging reader (FUJIBAS 1800). Analysis were performed for 3 h at room temperature with vacuum. The degree of crystallinity ($\chi_c$) was evaluated from radial scans of the X-ray diffraction images of unoriented samples, by applying the standard procedure of resolving the diffraction pattern into two areas, $A_c$ and $A_a$, that can be taken as proportional to the crystalline and the amorphous fraction, respectively, and calculated, for the $2\theta$ range 5–35°, using the equation (eq. (1))

$$x_c = \frac{A_c}{A_c + A_a} \times 100 \tag{1}$$

according to the classical Hermans-Weidinger method [82].

The degree of axial orientation relative to the crystalline phase has been formalized on a quantitative numerical basis using the Hermans' orientation function [83–85]:

$$f_{c,RX} = \left(3\overline{\cos^2 x} - 1\right)\Big/2 \tag{2}$$

by assuming $\overline{\cos^2 x}$ as the squared average cosine value of the angle, $x$, between the draw direction and the crystallographic $c$ (chain) axis. The orientation factor, $f_c$, is equal to 1 for perfect alignment ($x = 0°$), whereas it is equal to −0.5 for perpendicular alignment ($x = 90°$). For random orientation $\overline{\cos^2 x}$ is 1/3 and hence $f_c$ is zero.

Since for poly(isoprene-1,4-cis) an intense and isolated (200) reflection is present, the quantity $\overline{\cos^2 x}$, and hence the degree of axial orientation $f_{c,RX}$, can be experimentally evaluated by:

$$\overline{\cos^2 x} = \overline{\cos^2 \chi_{200}} = \frac{\int_0^{\pi/2} I(\chi_{200}) \cos^2 \chi_{200} \sin \chi_{200} d\chi_{200}}{\int_0^{\pi/2} I(\chi_{200}) \sin \chi_{200} d\chi_{200}} \tag{3}$$

where $I(\chi_{200})$ is the intensity distribution of the 200 diffractions on the Debye ring (at $2\vartheta_{CuK\alpha} = 13.8°$) and $\chi_{200}$ is the azimuthal angle measured from the equator.

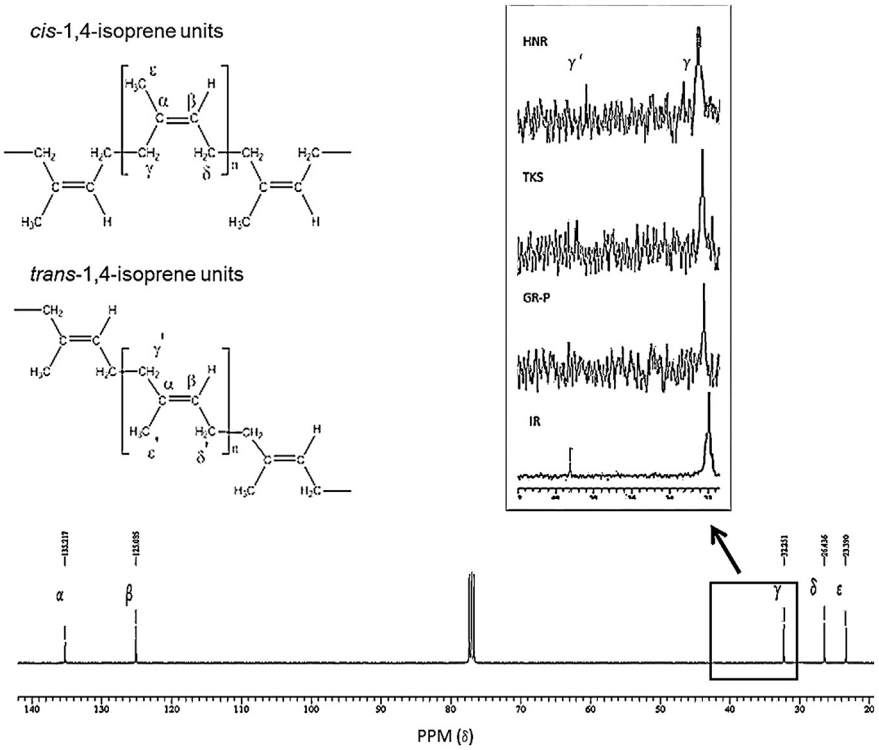


**Fig. 1.** $^{13}C$-NMR spectra (100 MHz in $CDCl_3$) of poly(isoprene) samples. The inset enlarges the range from 31 to 42 ppm, with the peak corresponding to the $\gamma^1$ carbon.

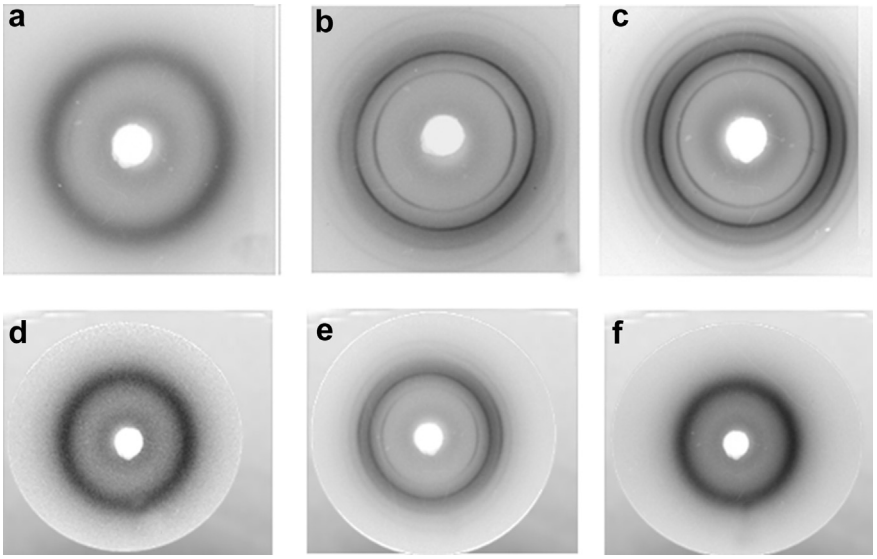


**Fig. 2.** WAXD photographic patterns of unstretched samples of TKS (a), HNR-L-C (b), HNR-H, GR-R (d), GR-P (e) and IR (f).

The diffracted intensities $\boldsymbol{I}(\chi_{200})$ were obtained by using digital imaging reader (FUJIBAS 1800) on photographic patterns like those of Fig. 2.

*Quasi static properties.* Tensile tests were carried out at room temperature by means of a dynamometer (Zwick Roell Z010) with optical extensometer. The clamps rate was 1 mm/min and the chamber load was 10 kN. (ISO 37/UNI 6065).

## 3. Results

### *3.1. Chemical composition of rubber samples and molecular features poly(isoprene)s*

Content of non rubber components was determined for HNR, GR, TKS and IR samples. Determination was performed by means of TGA and extraction with acetone [31,48], carried out under nitrogen and in the absence of light, to avoid modification of the chemical nature of NR components. Indeed, thermal and oxidative degradation of NR has been documented, in particular for GR [86–89].

Content of non rubber components and characteristics of poly(isoprene) samples are shown in Table 1. Data reveal that the raw sample of G-NR (GR-R) contains remarkably larger content of by products (about 9% by mass), whereas lower and similar amount was found for TKS and HNR, 3% and 2% by mass respectively. As expected, non rubber components were undetectable in synthetic poly(isoprene).

The amount of non rubber components detected in HNR samples appear slightly lower than the one reported in the scientific literature. In fact, acid coagulated HNR was reported to contain about 6% by mass of the following non rubber chemicals: neutral lipids (2%), glycolipids and phospholipids (1%), proteins (2%), carbohydrates (0.5%), ash (0.2%), and others (0.1%) [3–78]. About 3.5% of by products were obtained from acetone extraction of standard HNR grade (TSR 20) [31]. It is acknowledged that the chemical composition of NR from the Russian dandelion (TKS) and from guayule (G-NR) depends not only on the plantation but also on harvesting and processing procedures. The extraction technique as well remarkably affects the amount of extracted products. Non rubber components were about 6% in GR ASTM 2227 grade 5 [37]. The maximum amount of resins extracted with acetone was found to be about 8% in GR from two year-old guayule plants grown in Arizona [90] and from 3 to 4 year-old plants from Yulex [48]. Resins mainly contained terpenoids and fatty acid triglyercides, lipids, pigments. Acetone extractables in *taraxacum kok-saghyz* grown in USA in 1940s were 7% [30] and were about 4% in TKS harvested in Kazakhistan [31].

Polymer characteristics were determined on raw samples and, in the case of GR, also on the sample purified (GR-P) via extraction

**Table 1**
Content of low molar mass components and characteristics of PI samples.

| | Sample of poly(1,4-*cis*-isoprene) | | | | | |
|---|---|---|---|---|---|---|
| | HNR-H | HNR-L | TKS | GR-R | GR-P | IR |
| Low molar mass components (mass%) | | | | | | |
| from TGA | 2.1 | 1.7 | 3.1 | 8.9 | 1.5 | ~0 |
| from extraction with acetone[a] | 1.8 | 1.6 | 2.8 | 12 | 0.7 | ~0 |
| Mw[b] $10^{-6}$ (Da) | 2.3 | 1.5 | 1.4 | n.d. | 2.5 | 1.1 |
| Mw/Mn[b] | 3.3 | 3.2 | 1.8 | n.d. | 3.2 | 3.4 |
| Mooney Units[c] | 99 | 73 | 76 | 35 | 102 | 70 |
| Tg[d] (°C) | −64.9 | - 64,4 | - 64,9 | - 64,6 | - 64,9 | −65,3 |
| 1,4-*cis* units[e] (mol %) | n.d. | 98.8 | 100.0[f] | n.d. | 99.2 | 98.3 |

[a]Extraction Procedure: ISO1407 [b]from GPC analysis [c]from Mooney measurements [d] from DSC [e]from $^{13}$C NMR 100 MHz [f]signals due to repeating units other than 1,4-cis were undetectable.

with ethyl acetate. All of poly(isoprene)s have high molar mass ($M_w$ higher than $10^6$ Da) and comparable molar mass distribution ($M_w/M_n$ equal to about 3). It is known that HNR, GR and TKS can have high molar mass. $M_w$ as high as 2.5 $10^6$ Da was reported for standard HNR grade (TSR 20) with 1.3 as $M_w/M_n$ [31]. GR extracted from bark and wood of 50-month-old plants grown in California were found to have Mw in the following ranges: from $2.9 \times 10^5$ to $1.2 \times 10^6$ and from $1.7 \times 10^5$ to $6.1 \times 10^5$ respectively [90]. GR had Mw from 6.1 $10^4$ to 1.1 $10^6$ when it was from Mexican plants [91] and about 7.2 $10^5$ Da, with Mw/Mn equal to 4.4, when it was from greenhouse-grown two years old plants [92]. TKS harvested in Kazakhistan had Mw equal to $1.8 \times 10^6$ Da, with 1.6 as Mw/Mn [31].

Glass transition temperature (Tg) was found at about − 65 °C. Steric purity was assessed through $^{13}C$-NMR analysis [93,94]. The NMR spectrum of *HNR* is shown in Fig. 1. In the inset, the expanded region between 31 and 42 ppm is reported: Peaks, with normalized intensity, are due to 1,4-*cis* units (32.2 ppm) and to 1,4-*trans* units (39.7 ppm) for the $\gamma$ and $\gamma^1$ carbon, respectively. TKS reveals the highest stereoregularity: repeating units other than 1,4-*cis* are undetectable. All of the other poly(isoprene)s have high 1,4-*cis* content, about 98%, with slightly lower stereoregularity for the IR sample.

Nitrogen content, chemical nature and relative amount of low molar mass components of poly(isoprene)s from natural sources were also investigated. Data are in Table 2.

The nitrogen content, determined through elemental analysis, was taken as indication of the amount of proteins. Data collected in Table 2 show that the highest nitrogen content, from about 0.3 to about 0.5 as mass%, was found in HNR samples and was appreciably lower in the other rubbers. These findings appear in line with the value reported in the literature for the nitrogen content in solid rubber, 0.4% [79], and in the fresh latex, about 2% [3], taking into account that only about 25% of proteins in fresh hevea latex are adsorbed on rubber particles. 4.3% and 0.96% of proteins were found in fresh and centrifuged HNR latexes, respectively [95]. Low nitrogen content (≤0.6 mass %) was reported for the GR ASTM 2227 grade 5 and for a FEMA specification grade [38,39]. The nitrogen content was found lower (from 0.16 to 0.3 mass %) in mexican GR pilot plant grades than in HNR [37]. It is known that water-soluble proteins are known to be allergenic, potentially leading to anaphylactic shock [77,95,96]. In a recent work [97], the proteome of HNR latex has been explored via combinatorial peptide ligand libraries, identifying 300 unique gene products. Deproteinized HNR samples are available, containing about 0.02% nitrogen content.

GC-MS, $^1H$ NMR and $^{13}C$ NMR analyses were performed on non rubber products obtained through the extraction of NR samples with acetone. Major components were fatty acids in the case of HNR and TKS, whereas they were in a very minor amount in the sample from GR. Amount and chemical composition of fatty acids mixture is shown in Table 2. The largest amount of fatty acid was found in TKS, in particular unsaturated fatty acids. Linoleic and linolenic acids were in larger amount in HNR samples. This is in line with what reported in the literature [3]. Minor amount of unsaturated acids was found in GR samples, whereas the saturated acids were undetectable. The highest relative amount of saturated fatty acids, such as palmitic and stearic, was found in HNR. By products present in large amount in GR-R were undetectable in NR samples from other natural sources. Such chemicals were unsaturated, with iodine number equal to 44%. $^{13}C$ NMR analysis revealed that these products are sesquiterpenes. Their relative abundance is presented in Table 3.

**Table 3**
Relative abundance of terpenes present in GR sample.

| Chemical | Relative abundance[a] |
|---|---|
| Argentatines | 70 |
| Guayuline A | 50 |
| Guayuline B | 30 |
| Beta-phellandrene | 6 |
| cadinene | 5 |
| eudesmol | 1 |

[a] eudesmol = 1.

The presence in GR samples of a prevailing amount of argentatines and guayulines has been reported in the literature [98]. The concentration of sesquiterpenes in the essential oil of parthenium argentatum leaves was determined to be 39.5% [99]. Steam distillation of the leaves led to identify monoterpenes such as, mainly, α-pinene and β-pinene, and then terpinolene, sabinene, limonene, camphene, β-myrcene and β-ocimene. The absence of monoterpenes in GR sample studied in the present work could be ascribed to the procedure adopted for isolating the rubber from the GR latex. Moreover, as mentioned in the introduction, it is widely acknowledged that the chemical composition of GR depends on crops and on latex processing conditions.

Data in Tables 2 and 3 show appreciable differences among the chemical compositions of poly(isoprene)s samples.

### 3.2. Crystallinity in unstretched NR samples

Crystallinity in unstretched samples was studied for H-NR, TKS and GR samples, by means of WAXD analysis. In particular, HNR samples had high and low molar mass (HNR-H and HNR-L) and GR samples were as precipitated from the latex (GR-R) and after extraction with solvent (purified, GR-P).

Unstretched plates (about 0.5 mm thick) were prepared passing the rubber samples between the rolls of the two roll mill and pressing then the sheets under a pressure of about 0.35 MPa. Stretching was up to $\alpha = 5$ as the strain ratio. The WAXD photographic patterns of 0.5 mm thick NR plates, before stretching, are

**Table 2**
Nitrogen content and chemical composition of free fatty acids mixture in NR samples.

| | HNR-H | HNR-L | TKS | GR-R | GR-P |
|---|---|---|---|---|---|
| Nitrogen content (mass %)[a] | 0.47 | 0.28 | 0.15 | 0.04 | 0.03 |
| Fatty acids (mass %)[a] | | | | | |
| total amount | 1.12 | 1.53 | 2.87 | 0.6 | 0.91 |
| C16 - Palmitic | 0.12 | 0.33 | ~0 | ~0 | ~0 |
| C18 - Stearic | 0.18 | 0.32 | 0,53 | ~0 | ~0 |
| C18:1 - Oleic | 0.20 | 0.20 | 0,43 | 0.02 | ~0 |
| C18:2 - Linoleic | 0.57 | 0.61 | 1,76 | 0.38 | 0.60 |
| C18:3 - Linolenic | 0.05 | 0.06 | 0,14 | 0.17 | 0.19 |
| Saturated - Unsaturated | 0.3–0.82 | 0.65–0.88 | 0.53–2.33 | ~0–0.58 | ~0–0.79 |

[a] On the total mass of the rubber sample.

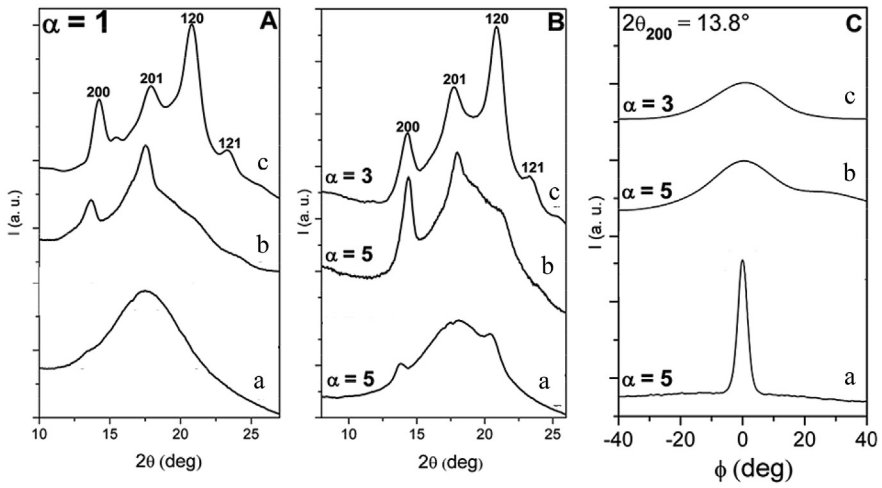


**Fig. 3.** WAXD patterns corresponding to equatorial (A, B) and azimuthal (C) scans of photographic patterns of: (A) unstretched samples of Fig. 2; (B, C) axially stretched samples of Fig. 6a–d. The azimuthal scans (C) are collected for the 200 reflection at $2\vartheta_{CuK\alpha} = 13.8°$. The $\alpha$ value indicates the ratio between final and initial sample length. The samples are: (a) TKS, (b) HNR-L-C, (c) HNR-H.

shown in Fig. 2. They are from the following NR samples: TKS (a), HNR-L-C (b), HNR-H (c), GR-R (d), GR-P (e) and IR (f).

Additional information relative to the diffraction of the unstretched and stretched NR samples were obtained from the equatorial scans of the photographic patterns of Fig. 2 (except IR). They are shown in Fig. 3A for TKS(a), HNR-L-C (b), HNR-H (c) and are shown in Fig. 4 for GR-P (d) and GR-R (e).

Inspection of Figs. 2, Figs. 3 and 4 allows the following comments.

At $\alpha = 1$, HNR-H, HNR-L-C and GR-P are crystalline, whereas TKS, GR-R and IR are amorphous. Larger crystallinity is definitely shown by HNR-H plates. Many intense Debye rings are in the WAXD pattern of Fig. 2a and the patterns of Fig. 4A indicate that the degree of crystallinity $\chi_c$ is 18%. Both these patterns and the equatorial scan (Fig. 3A(d)) reveal 200, 201, 120 and 121 reflections, with the usual relative intensities [100–105] and maximum intensity for the 120 reflection (at $2\theta = 21.2°$). It has been reported [47] that aging at room temperature (for 6 months) of HNR-H plates led to the increase of crystallinity, up 30%, with a melting temperature of about 45 °C, surprisingly high, taking into consideration the values reported in the literature: from DSC measurements, experimental values were always lower than 25 °C [106–108]. Melting point higher than 40 °C has been reported only when measurements were performed under a pressure higher than 1.5 kbar [109].

HNR-L sample revealed a peculiar behaviour. It was amorphous before processing and, after passing through the two roll mill, either remained amorphous or developed a partial crystallinity, as revealed by some Debye rings due to crystalline reflections of poly(1,4-cis-isoprene) [1]. The disordered crystalline modification was unusual, with 120 and 121 reflections having low intensity, and was unstable at room temperature. In a recent work by the authors [47], both the amorphous and the crystalline samples have been presented. Rationalization for the occurring of crystallinity was on the basis of a crystalline packing, with disorder mainly along the *b* axis. It has been reported that the crystallinity of HNR-L-C was lost after aging at room temperature for 6 months. To underline that the crystalline sample has been selected for the present work and to allow an easier comparison with the mentioned work [47], the label HNR-L-C has been adopted.

The GR-P sample (the GR-R sample after solvent extraction) showed partial crystallinity, which was estimated of about 10%.

TKS and GR-R were found completely amorphous, whatever the processing conditions.

### 3.3. Crystallinity in stretched NR samples

The development of crystallinity and mechanical reinforcement under axial stretching was studied for the same samples. The WAXD photographic patterns of 0.5 mm thick plates, upon stretching at $\alpha = 5$, are shown in Fig. 5. Patterns are from the following NR samples: TKS (a), HNR-L-C (b), HNR-H (c), GR-R (d), GR-P (e) and IR (f) samples.

The corresponding equatorial scans and azimuthal scans (for the 200 reflection at $2\vartheta_{CuK\alpha} = 13.8°$) are shown in Fig. 3B(a-c) and

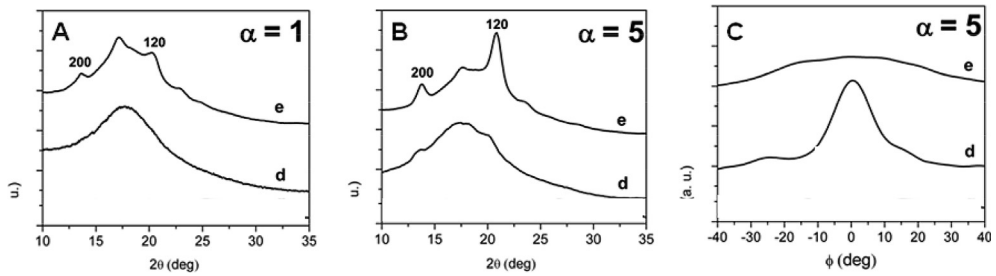


**Fig. 4.** WAXD patterns corresponding to equatorial (A,B) and azimuthal (C) scans of photographic patterns of: (A) unstretched samples of Fig. 2; (B,C) axially stretched samples of Fig. 6a–d. The azimuthal scans (C) are collected for the 200 reflection at $2\vartheta_{CuK\alpha} = 13.8°$. The $\alpha$ value indicates the ratio between final and initial sample length. The samples are: (d) GR-R, (e) GR-P.

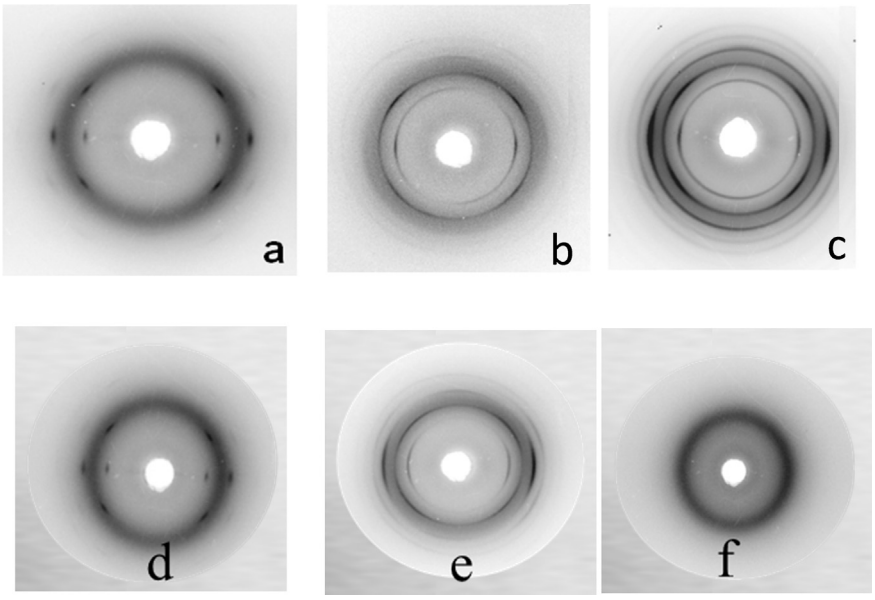


**Fig. 5.** WAXD photographic patterns of samples of TKS (a), HNR-L-C (b), HNR-H, GR-R (d), GR-P (e) and IR (f) stretched at $\alpha = 5$.

Fig. 3C(a-c) for the TKS and HNR samples and in Fig. 4B(d-e) and Fig. 4C(d-e) for GR samples, respectively.

As reported in the previous paragraph, TKS, GR-R and IR were amorphous after processing and at $\alpha = 1$.

Among these amorphous samples, only TKS was able to develop crystallinity under strain: strain induced crystallization occurred only for $\alpha > 4$. TKS sample stretched at $\alpha = 5$ shows narrow peaks in the azimuthal scans of Fig. 3C (a), thus indicating the formation of crystalline phase with high degree of axial orientation ($fc = 0.95$).

GR-R and IR were not able to develop crystallinity.

The HNR-L-C sample, moderately crystalline at rest, developed a low degree of axial orientation (maximum value of $fc = 0.69$). Indeed, large diffraction arcs are present in Fig. 2 and broad peaks are in the azimuthal patterns of Fig. 3A. Moreover, a slight increase of crystallinity was observed, as it is revealed by the comparison of pattern (a) in Fig. 3A and B. It is worth commenting that the anomalous crystallinity, observed in processed plates, was maintained also after stretching.

### 3.4. Crystallization and reinforcement under strain

The stress–strain curves from quasi-static measurements taken on HNR-L-C, TKS, GR-R, GR-P and IR are shown in Fig. 6.

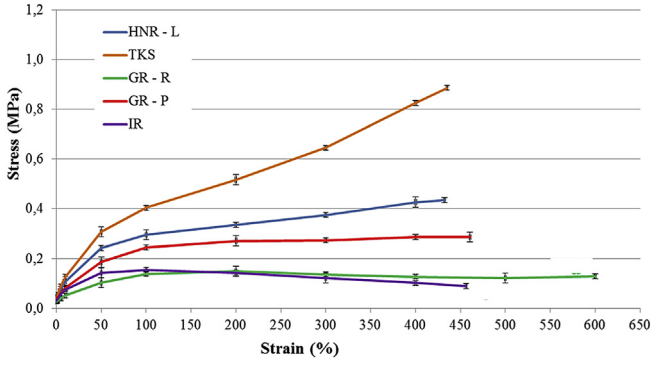


**Fig. 6.** Nominal stress/nominal strain curves obtained for HNR-L-C, TKS, GR-R, GR-P and IR.

Reinforcement under strain was not observed for IR.

GR-P achieved larger stress values than GR-R. As reported above, GR-R is able to form oriented crystallites under strain. GR-P and HNR-L-C are crystalline after processing at $\alpha = 1$. They are not able to give rise, under stretching, to an appreciable increase of crystallinity. Clear reinforcement is shown by the TKS sample, which has higher stress values at all deformations with respect to all the other samples, in particular at large strains. TKS is amorphous at rest and is able to form oriented crystallites under strain.

The different behaviour of poly(isoprene)s samples from different natural sources was investigated focusing the attention on those which revealed the larger reinforcement under strain: HNR-L-C and TKS. Photographic WAXD patterns were collected during stretching at different draw ratios and they are reported in Fig. 7 for HNR-L-C and in Fig. 8 for TKS ($\alpha$ values are shown close to the curves).

The inspection of the graphs in Fig. 7 and in Fig. 8 reveals that crystallinity does not remarkably increase under stretching in the case of HNR-L-C, whereas, for TKS sample, oriented crystalline phase is revealed at $\alpha = 4.5$ and is further developed at $\alpha = 5$.

### 3.5. Study of the effect of poly(isoprene) molar mass

The effect of molar mass on crystallization and reinforcement under strain was investigated on HNR-H, that means the NR sample

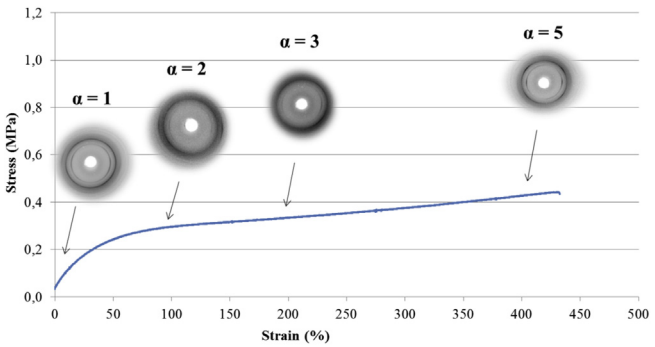


**Fig. 7.** Room temperature nominal stress – nominal strain curves for HNR-L-C sample.

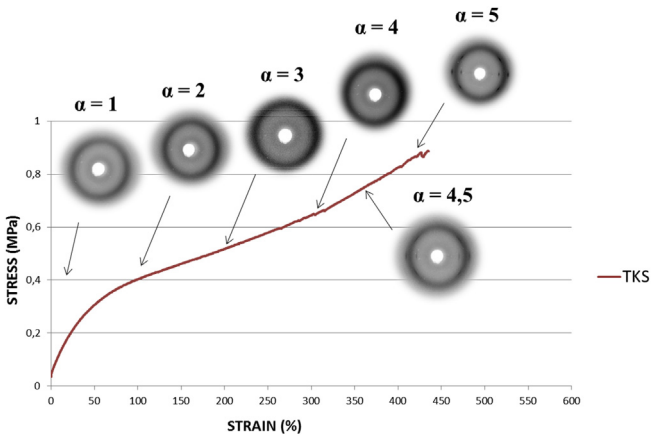


**Fig. 8.** Room temperature nominal stress – nominal strain curves for TKS sample.

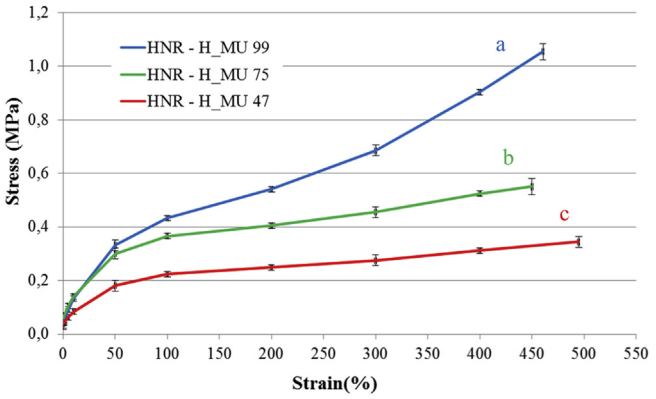


**Fig. 11.** Nominal stress/nominal strain curves obtained for HNR samples with 99 (a), 75 (b) and 47 (c) Mooney units, as the molar mass index.

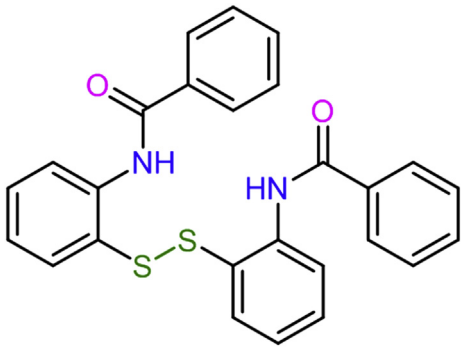


**Fig. 9.** Dibenzamido diphenyldisulphide.

from *Hevea Brasiliensis* with higher molar mass. The molecular feature of this poly(isoprene) sample and the content of low molar mass components are in Table 1. Nitrogen content and composition of free fatty acids mixture are in Table 2.

HNR-H was melt blended with two different contents, 0.05 and 0.1 as mass %, of dibenzamido diphenyldisulphide, a chemical whose chemical structure is in Fig. 9.

Reduction of molar mass was expected, as the disulfide is able to trap the chain end radicals generated by the thermomechanical blending. The molar masses of the three HNR specimens were determined by means of Mooney measurements and were found to correspond to 99, 75 and 47 Mooney units, for starting HNR-H and for the samples blended with 0.05 and 0.1 as mass% of disulfide, respectively. WAXD patterns were taken on samples stretched to the largest strain ratio, $\alpha = 5$, to allow the development of the largest amount of crystallinity. The 2D diffraction patterns of HNR-H samples with different molar mass are shown in Fig. 10.

Crystallinity can be observed in the 2D patterns of the two HNR samples with higher molar masses, 99 and 75 as Mooney units, with higher content for the former one. HNR sample with 47 MU is completely amorphous. Oriented crystalline phase appears to be present in the sample with the highest molar mass.

The stress–strain curves obtained from quasi static tensile tests on the three samples of HNR are in Fig. 11.

Reduction of molar mass leads to a substantial decrease of stresses at every elongation. The sample with the lowest molar mass, amorphous at $\alpha = 5$, does not show appreciable reinforcement under strain.

### 3.6. Study of the effect of non rubber components

The effect of non rubber components was studied for both HNR and TKS samples. Solvent extraction of HNR was performed adopting the procedure reported in the experimental part, obtaining a specimen with almost undetectable amount of free fatty acids and with reduced nitrogen content (about 0,1%).

2D WAXD patterns of pristine (a) and extracted (b) HNR samples drawn at $\alpha = 1$ and at $\alpha = 5$ are shown in Fig. 12 and in Fig. 13, respectively.

It appears that the extraction of free fatty acids and free proteins from HNR led to the reduction of crystallinity. The stress–strain curves obtained from quasi-static measurements for the HNR sample, before (a) and after (b) extraction with solvent are shown in Fig. 14.

It appears that the extraction of fatty acids and proteins led to the reduction of stresses at all the elongation.

The effect of free and linked molecules on strain induced crystallization and reinforcement was investigated for the TKS sample. TKS was first extracted, as reported above for HNR, to remove free chemicals, essentially free fatty acids. The TKS sample without fatty

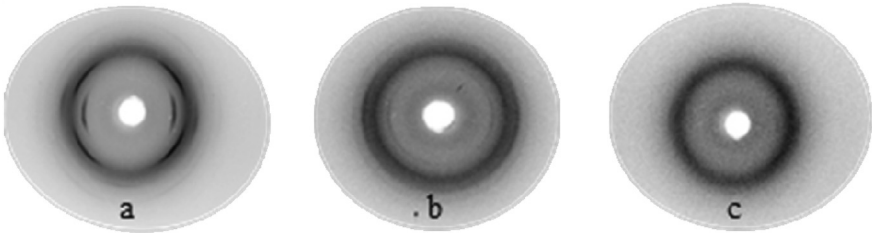


**Fig. 10.** 2D WAXD patterns of the HNR samples with 99 (a), 75 (b) and 47 (c) Mooney units, as the molar mass index, stretched at $\alpha = 5$.

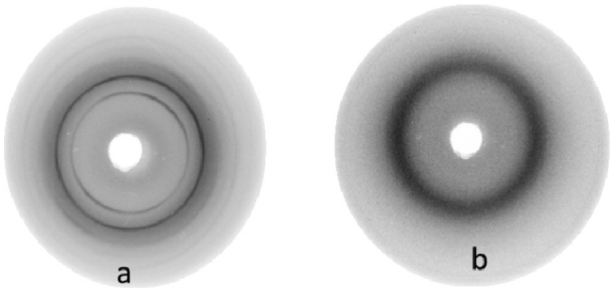


**Fig. 12.** WAXD patterns of pristine (a) and extracted (b) HNR samples drawn at $\alpha = 1$.

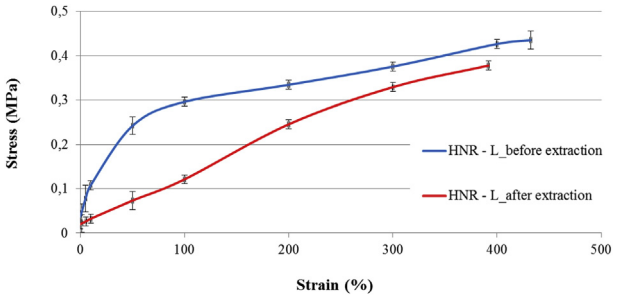


**Fig. 14.** Nominal stress/nominal strain curves obtained for HNR samples before (a) and after (b) extraction of fatty acids.

acids was reacted with sodium methoxide, to have trans esterification of the phospholipidic terminals and scission of the amidic bonds in proteins. 2D WAXD patterns of TKS samples, stretched at $\alpha = 5$ are shown in Fig. 15: after extraction (a) and after reaction with sodium methoxide (b).

Crystallinity with poor orientation is visible in the TKS sample after solvent extraction, whereas the specimen treated with sodium methoxide is completely amorphous. The stress–strain curves for TKS samples, pristine and after the treatment, are in Fig. 16.

It appears that remarkable reduction of stresses at all the elongations is caused by the extraction of fatty acids and that, in particular, reinforcement under strain cannot be detected for the sample which experienced the treatment with sodium methoxide.

To further investigate the effect of fatty acids, either stearic or linoleic acid were added to a HNR-L sample purified through extraction with acetone. Stearic acid should be a nucleating agent and linoleic acid should be a plasticizer. 2D WAXD patterns of HNR-L samples are in Fig. 17.

Quasi static properties after addition of stearic acid and linoleic acid are in Fig. 18.

The addition of stearic acid does not promote the crystallization of the HNR sample obtained after purification. Instead, it is possible to observe the increase of the stresses at all the elongations.

The addition of linoleic acid does not promote the crystallization and mechanical reinforcement of the HNR sample obtained after purification.

## 4. Overall discussion of results

A correlation cannot be established between stereoregularity and crystallinity of the unstretched samples, after processing, at $\alpha = 1$. In fact, TKS, which has the highest steric purity, is amorphous at $\alpha = 1$. HNR-H and HNR-L have different degree of crystallinity, but the stereoregularity of these samples appears to be very similar. The lower stereoregularity could be at the origin of the absence of crystallinity at $\alpha = 1$ of the IR sample, which is also not able to develop crystallinity under stretching. However, it has to be considered that chain end crosslinking, which is acknowledged to play a key role in promoting the SIC phenomenon [72–79], is absent in the synthetic poly(isoprene).

The molar mass of poly(isoprene) seems to have a remarkable effect on crystallinity of unstretched samples and, particularly, on the crystallization and reinforcement under stretching. It could be hypothesized that the high molar mass could be beneficial for the larger amount of crystallinity at $\alpha = 1$ of HNR-H, if not from the kinetic point of view, at least reducing the effect of chain ends. GR-P, which is crystalline at $\alpha = 1$, has high molar mass, even higher than HNR-H. The 2D WAXD patterns of HNR-H samples treated with increasing amount of 2,2′-dibenzamido diphenyl disulfide and stretched at $\alpha = 5$ reveal the reduction of crystallinity in samples with lower molar mass and to the substantial decrease of stresses at every elongation. The role of molar mass on the induction of crystallization has been highlighted in recent works [72,110]. Entanglements have been found to promote chains alignment and to induce the formation of crystals in IR at low temperatures (0, −25 and −50 °C). At 25 °C, entanglements led to a viscous response with yield stress but without crystallization under strain. HNR showed instead crystallization and reinforcement under strain also at 25 °C. It was commented that the pseudo end-linked polymer chains network, present in HNR, made permanent the entanglements.

A clear effect on crystallinity and crystallization and reinforcement under stretching is played by non rubber components. GR-R is amorphous after processing at $\alpha = 1$ and this can be attributed to the large amount of terpenes. GR-P, that means GR-R after extraction of terpenes, is crystalline at $\alpha = 1$. Terpenes could thus act as plasticizers for GR-R. GR-R is able to develop oriented crystallinity under stretching, but not reinforcement. It seems that the amount of terpenes is beneficial for allowing amorphous chain to align themselves under strain but is too high to allow appreciable enhancement of the mechanical properties.

The prevailing content of unsaturated fatty acids (which are above their melting temperature, at RT) in TKS could prevent crystallization at $\alpha = 1$. Unsaturated fatty acids could act as

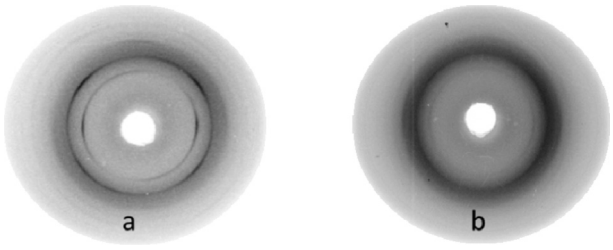


**Fig. 13.** 2D WAXD patterns of pristine (a) and extracted (b) HNR samples drawn at $\alpha = 5$.

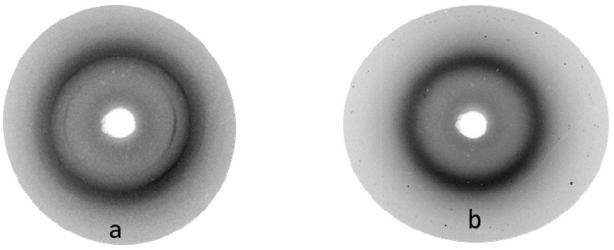


**Fig. 15.** 2D WAXD patterns of TKS samples, stretched at $\alpha = 5$: after extraction (a) and after reaction with sodium methoxide (b).

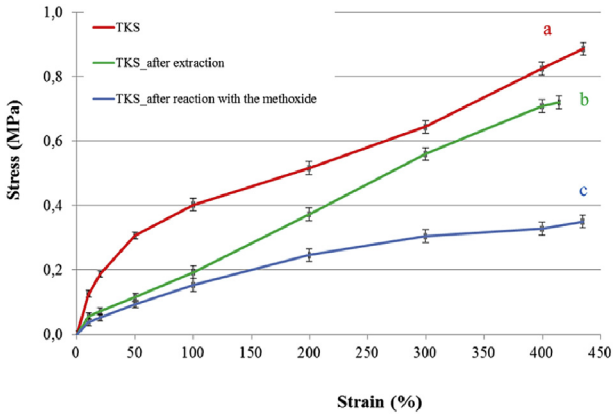


**Fig. 16.** Nominal stress/nominal strain curves obtained for TKS samples: raw (a), after extraction (b) and after reaction with sodium methoxide (c).

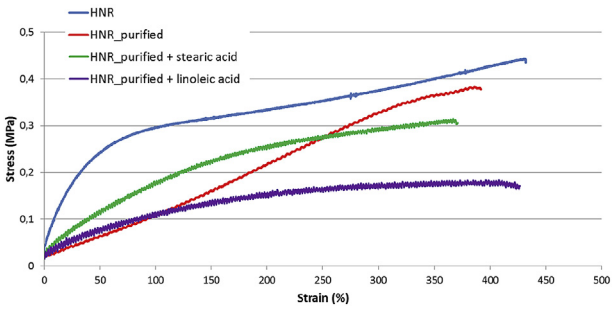


**Fig. 18.** Nominal stress – nominal strain curves for HNR-L samples: as such, purified, after the addition of stearic or linoleic acids.

plasticisers for TKS. The addition of linoleic acid to TKS leads to the reduction of reinforcement under strain.

The large crystallinity of HNR-H could be also ascribed to the presence of saturated fatty acids, which have been reported to act as nucleating agents [75], though it is indeed a difficult task to identify nucleating agents in a complex mixture such as the one of non rubber components. The lower crystallinity of GR-P could be also ascribed to the absence of fatty acids. It was shown in Figs. 12, Figs. 13 and 14 (for the HNR sample) and in Figs. 15 and 16 (for TKS sample) that the removal of free fatty acids and proteins led to appreciable reduction of crystallization and reinforcement under strain. The role of free saturated fatty acids and proteins in promoting crystallinity is widely acknowledged. It was reported that the rate of HNR crystallization, after removal of free fatty acids, was brought back to the original level by adding 1% of stearic acid [75,111] and that a mixture of saturated fatty acids accelerate the crystallization of IR [74]. The effect of fatty acids on the crystallization behaviour of HNR was commented to be larger than that of proteins [75]. However, proteins are known to promote the storage hardening of NR [3,40], which could be due to the crosslinking reaction promoted by proteins with oxygenated functional groups assumed to be on rubber chains. De-proteinized HNR required the highest strains for inducing crystallization [38] and the green strength of the rubbers was found to decrease in samples with undetectable amount of proteins [79,112]. Interestingly, results here reported (Figs. 17 and 18) show that a saturated fatty acid (such as stearic acid) has preferential effect on reinforcement rather than on crystallization under strain, when added in small amount to acetone extracted HNR sample. It seems that the saturated fatty acid has effect on the mechanical reinforcement rather than on the crystallization ability of the HNR sample.

Chain end crosslinking has indeed a great effect on crystallinity and crystallization under stretching. TKS after the treatment with sodium methoxide does not show crystallization and reinforcement under strain. As mentioned above, the absence of chain end crosslinking in synthetic poly(isoprene) cannot be disregarded to explain its amorphous nature at $\alpha = 1$ and the absence of crystallization and reinforcement under stretching.

Results of the present work draw the attention on the behaviour of NR samples under stretching. GR-R and, in particular, TKS developed oriented crystalline phases under stretching and only TKS was able to show reinforcement under strain. Lower green strength was reported in the literature [34] for GR with respect to HNR, with consistent reduction as the amount of resins in the GR sample increased (from 1 to 9%). In the mentioned work, information is not available on crystallization. Better failure properties were reported [37] for cured GR with 3–4% of by products, with respect to HNR having the same amount of non rubber molecules, but also with respect to cleaner or deproteneized HNR. This result was commented [38,40] to be unexpected, as it is known that more non rubber contaminants mean larger intrinsic flaws that should concentrate stress, promoting fracture and fatigue. It was thus hypothesized [40] that non rubber contaminants nucleate crystallization. Results of the present work allow to propose an alternative hypothesis. The formation of oriented crystalline phase with the increase of $\alpha$, in TKS and GR-R, arises from the strain induced orientation of the amorphous phase, which generates highly oriented crystallites. Crystallization involves chains that are mostly oriented along the stretching direction. The large development of oriented crystallinity and reinforcement in the case of TKS could be reasonably correlated with the high stereoregularity of such poly(isoprene). Semicrystalline polymer such as poly(-ethyleneterephtalate) (PET) was reported, by one of the authors [113], to develop analogous phenomenon. PET fibers with higher content of diethylene glycol revealed a delayed crystallization, that allowed the progress of the amorphous phase orientation and, in turns, the formation of oriented crystallites and the development of higher tenacity. Reinforcement under stretching of NR samples is due to the crystalline phase and is stronger when the crystallization occurs at high draw ratios: highly oriented chains form highly oriented crystalline phase.

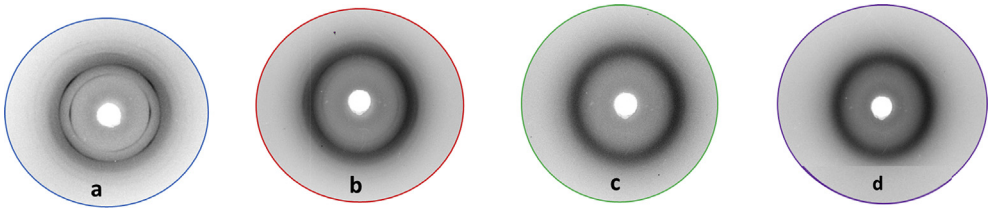


**Fig. 17.** 2D WAXD patterns at $\alpha = 5$ of HNR-L: as such (a), after solvent extraction (b), after addition of stearic acid (c), after addition of linoleic acid (c).

## 5. Conclusions

Strain induced crystallization and reinforcement are at the origin of outstanding properties of natural rubber such as very high tensile strength and crack growth resistance. This work investigated crystallization and reinforcement under strain in uncrosslinked poly(1,4-cis-isoprene)s samples from Ziegler–Natta catalysis and from different natural sources: *hevea brasiliensis*, *partenium argentatum* and *taraxacum kok-saghyz*. For the first time, comparison is performed among NR samples from all these sources.

Crystallinity was found in processed, unstretched (strain ratio $\alpha = 1$) plates of HNR-H and GR-P, that means two samples with high molar mass and with limited amount or absence of non rubber components. HNR-L, with low molar mass, showed a low and unstable crystallinity. TKS and GR-R were amorphous.

The largest reinforcement under strain was obtained with TKS, that means with a sample amorphous at $\alpha = 1$. Crystallization started at high draw ratios and highly oriented crystallites were formed. The positive effect on SIC of pseudo end-linked polymer chains network is shown for TKS, which did not show any crystallization and reinforcement under strain after the reaction with a reagent such as sodium methoxide, able to promote transesterification reaction of polymer chain ends and cleavage of proteins bonds. It can be hypothesized that positive effect on these results came also from non rubber components such as unsaturated fatty acids, which could act as plasticizers, preventing crystallization at $\alpha = 1$.

Oriented crystallites were shown also by the GR-R sample, in minor amount with respect to TKS. Terpenes appear to act as plastifiers for GR-R, preventing crystallization at $\alpha = 1$ and the development of reinforcement upon stretching.

HNR and GR-P were crystalline at $\alpha = 1$ and did not reveal oriented crystallites under strain, with appreciably lower stresses at all the elongations with respect to TKS.

IR remained amorphous, without showing reinforcement, under stretching.

TKS, at least the sample analyzed in the present work, appears to be the ideal poly(isoprene) for achieving mechanical reinforcement and better failure properties, thanks to its ability to develop highly oriented crystallites and thus high reinforcement.

## Conflict of interest

The authors declare no conflict of interest.

## References


[1] C.W. Bunn, Proc. Royal Soc. London. Ser. A. Math. Phys. Sci. 180 (1942) 40–66.
[2] G. Natta, G. Allegra, Stereochemical aspects of crystalline synthetic macromolecules, Tetrahedron 30 (1974) 1987–2000.
[3] A.H. Eng, E.L. Ong, Hevea natural rubber handbook of elastomers, CRC Press, 2000, pp. 29–60.
[4] F.W. Barlow, Basic elastomer technology, Rubber Division American Chemical Society, 2001, pp. 235–258 [Chapter 9].
[5] Natural rubber statistics, 2016. http://www.lgm.gov.my/nrstat/nrstats.pdf.
[6] P.E. Hurley, History of natural rubber journal of macromolecular science: part a - chemistry 15 (7) (1981) 1279–1287.
[7] D. Hosler, S.L. Burkett, M.J. Tarkanian, Prehistoric polymers: rubber processing in ancient mesoamerica science 284 (5422) (1999 Jun 18) 1988–1991.
[8] M.J. Tarkanian, D. Hosler, America's first polymer scientists: rubber processing, use and transport in mesoamerica, Latin Am. Antiq. 22 (4) (2011) 469–486.
[9] C. Slack, Noble obsession: Charles goodyear, thomas hancock and the race to unlock the greatest industrial secret of the 19th century paperback, August 13, 2003.
[10] S. Kawahara, Y. Isono, J.T. Sakdapipanich, Y. Tanaka, E. Aik-Hwee, Effect of gel on the green strength of natural rubber, Rubber Chem. Technol. 75 (2002) 739–746.
[11] S. Amnuaypornsri, J. Sakdapipanich, Y. Tanaka, Green strength of natural rubber: the origin of the stress–strain behavior of natural rubber, J. Appl. Polym. Sci. 111 (2009) 2127–2133.
[12] G.R. Hamed, Tack and green strength of NR, SBR and NR/SBR blends, Rubber Chem. Technol. 54 (1981) 403–414.
[13] G.R. Hamed, Tack and green strength of elastomeric materials, Rubber Chem. Technol. 54 (1981) 576–595.
[14] R.P. Wool, Molecular aspects of tack rubber, Chem. Technol. 57 (1984) 307–319.
[15] A.G. Thomas, J.M. Whittle, Tensile rupture of rubber, Rubber Chem. Technol. 43 (1970) 222–228.
[16] A.N. Gent, L.Q. Zhang, Strain-induced crystallization and strength of rubber, Rubber Chem. Technol. 75 (2002) 923–934.
[17] W.F. Busse, Tear resistance and structure of rubber, Ind. Eng. Chem. 26 (1934) 1194–1199.
[18] S.M. Cadwell, R.A. Merrill, C.M. Sloman, F.L. Yost, Dynamic fatigue life of rubber, Ind. Eng. Chem. Anal. Ed. 12 (1940) 19–23.
[19] W.V. Mars, A. Fatemi, A literature survey on fatigue analysis approaches for rubber, Int. J. Fatig. 24 (2002) 949–961.
[20] W.V. Mars, A. Fatemi, Factors that affect the fatigue life of rubber: a literature survey, Rubber Chem. Technol. 77 (2004) 391–412.
[21] I.C. Papadopoulos, A.G. Thomas, J.J.C. Busfield, Rate transitions in the fatigue crack growth of elastomers, J. Appl. Polym. Sci. 109 (2008) 1900–1910.
[22] W.V. Mars, Computed dependence of rubber'S fatigue behavior on strain crystallization, Rubber Chem. Technol. 82 (2009) 51–61.
[23] N. Saintier, G. Cailletaud, R. Piques, Cyclic loadings and crystallization of natural rubber: an explanation of fatigue crack propagation reinforcement under a positive loading ratio, Mater. Sci. Eng. A 528 (2011) 1078–1086.
[24] G.J. Lake, Mechanical fatigue of rubber, Rubber Chem. Technol. 45 (1972) 309–328.
[25] G.R. Hamed, Molecular aspects of the fatigue and fracture of rubber, Rubber Chem. Technol. 67 (1994) 529–536.
[26] G.R. Hamed, H.J. Kim, A.N. Gent, Cut growth in vulcanizates of natural rubber, *cis*-polybutadiene, and a 50/50 blend during single and repeated extension, Rubber Chem. Technol. 69 (1996) 807–818.
[27] G.J. Lake, Fatigue and fracture of elastomers, Rubber Chem. Technol. 68 (1995) 435–460.
[28] G.R. Hamed, N. Rattanasom, Effect of crosslink density on cut growth in black-filled natural rubber vulcanizates, Rubber Chem. Technol. 75 (2002) 935–942.
[29] https://en.wikipedia.org/wiki/Damocles.
[30] R.K. Eskew, Natural rubber from Russian dandelion, Rubber Chem. Technol. 19 (1946) 856–864.
[31] A.U. Buranov, B.J. Elmuradov, Extraction and characterization of latex and natural rubber from rubber-bearing plants, J. Agric. Food Chem. 58 (2009) 734–743.
[32] F.E. Lloyd, Carnegie institution of Washington, 1911, p. 139.
[33] D. Spence, Rubber Chem. Technol. 1 (1928) 357.
[34] L.R. De Valle, M. Montelongo, Rubber Chem. Technol. 51 (1978) 863.
[35] T. Hager, A. MacArthur, D. McIntyre, R. Seeger, Rubber Chem. Technol. 52 (1979) 693.
[36] F.A. Eagle, Rubber Chem. Technol. 54 (1981) 662.
[37] I.S. Choi, C.M. Roland, Rubber Chem. Technol. 69 (1996) 591.
[38] I.S. Choi, C.M. Roland, Rubber Chem. Technol. 70 (1997) 202.
[39] W.W. Schloman Jr., F. Wyzgoski, D. McIntyre, K. Cornish, D.J. Siler, Rubber Chem. Technol. 69 (1996) 215.
[40] P.G. Santangelo, C.M. Roland, Rubber Chem. Technol. 74 (2001) 69.
[41] A.M. Bogacheva, G.N. Rudenskaya, A. Preusser, I.O. Tehikileva, Y.E. Dunaevsky, B.N. Golovskin, V.M. Stepanov, A new subtilisin-like proteinase from roots of the dandelion Taraxacum officinale Webb S. L, Biochemistry C/C of Biokhimiia 64 (1999) 1030–1037.
[42] H. Mooibroek, K. Cornish, Appl. Microbiol. Biotechnol. 53 (2000) 355–365.
[43] N. Dong, B. Montanez, R.A. Creelman, K. Cornish, Plant Cell. Rep. 25 (2006) 26–34.
[44] J.B. van Beilen, Y. Poirier, Crit. Rev. Biotechnol. 27 (2007) 217–231.
[45] J.B. van Beilen, Y. Poirier, Trends Biotechnol. 25 (2007) 522–529.
[46] C.S. Gronover, D. Wahler, D. Prüfer, Biotechnol. Biopolym. (2011) 75–88.
[47] Articolo su PAT Musto et al.
[48] K. Cornish, C.H. Pearson, D.J. Rath, Ind. Crop. Prod. 41 (2013) 158–164.
[49] J.H. Magill, Crystallization and morphology of rubber, Rubber Chem. Technol. 68 (1995) 507–539.
[50] M. Tosaka, Strain-induced crystallization of crosslinked natural rubber as revealed by X-ray diffraction using synchrotron radiation, Polym. J. 39 (2007) 1207–1220.
[51] B. Huneau, Strain-Induced Crystallization of natural rubber: a Review of X-ray diffraction investigations, Rubber Chem. Technol. 84 (2011) 425–452.
[52] R. Pérez-Aparicio, A. Vieyres, P.A. Albouy, O. Sanseau, L. Vanel, D.R. Long, P. Sotta, Reinforcement in natural rubber elastomer nanocomposites: breakdown of entropic elasticity, Macromolecules 46 (2013) 8964–8972.
[53] M. Hernández, M.A. López-Manchado, A. Sanz, A. Nogales, T.A. Ezquerra, Effects of strain-induced crystallization on the segmental dynamics of vulcanized natural rubber, Macromolecules 44 (2011) 6574–6580.
[54] J.R. Samaca Martinez, J.B. Le Cam, X. Balandraud, E. Toussaint, J. Caillard, Mechanisms of deformation in crystallizable natural rubber. Part 1: thermal characterization, Polymer 54 (2013) 2717–2726.

[55] K. Brüning, K. Schneider, G. Heinrich, Deformation and orientation in filled rubbers on the nano- and microscale studied by X-ray scattering, J. Polym. Sci. B Polym. Phys. 50 (2012) 1728–1732.
[56] J. Che, S. Toki, J.L. Valentin, J. Brasero, A. Nimpaiboon, L. Rong, B.S. Hsiao, Chain dynamics and strain-induced crystallization of pre- and post-vulcanized natural rubber latex using proton multiple quantum NMR and uniaxial deformation by in situ synchrotron X-ray diffraction, Macromolecules 45 (2012) 6491–6503.
[57] P.A. Albouy, G. Guillier, D. Petermann, A. Vieyres, O. Sanseau, P. Sotta, A stroboscopic X-ray apparatus for the study of the kinetics of strain-induced crystallization in natural rubber, Polymer 53 (2012) 3313–3324.
[58] M. Tosaka, K. Senoo, K. Sato, M. Noda, N. Ohta, Detection of fast and slow crystallization processes in instantaneously-strained samples of poly(-isoprene-1,4-cis), Polymer 53 (2012) 864–872.
[59] N. Candau, L. Chazeau, J.M. Chenal, C. Gauthier, E. Munch, Fall technical meeting of the rubber division ACS 182nd Cincinnati OH United States 3 (2012) 1936–1949.
[60] J. Che, C. Burger, S. Toki, L. Rong, B.S. Hsiao, S. Amnuaypornsri, J. Sakdapipanich, Crystal and crystallites structure of natural rubber and synthetic poly(isoprene-1,4-cis) by a new two dimensional wide angle X-ray diffraction simulation method. I. Strain-induced crystallization, Macromolecules 46 (2013) 4520–4528.
[61] J. Che, S. Toki, J.L. Valentin, J. Brasero, A. Nimpaiboon, L. Rong, B.S. Hsiao, Chain dynamics and strain-induced crystallization of pre- and post-vulcanized natural rubber latex using proton multiple quantum NMR and uniaxial deformation by in situ synchrotron X-ray diffraction, Macromolecules 45 (2013) 6491–6503.
[62] B. Heuwers, D. Quitmann, R. Hoeher, F.M. Reinders, S. Tiemeyer, C. Sternemann, J.C. Tiller, Stress-induced stabilization of crystals in shape memory natural rubber, Macromol. Rapid Commun. 34 (2013) 180–184.
[63] S.J. Mistry, S. Govindjee, A micro-mechanically based continuum model for strain-induced crystallization in natural rubber, Int. J. Solid Struct. 51 (2014) 530–539.
[64] R. Dargazany, V.N. Khiêm, E.A. Poshtan, M. Itskov, Constitutive modeling of strain-induced crystallization in filled rubbers, Phys. Rev. 89 (2014) 022604.
[65] C. Xu, Y. Chen, Y. Wang, X. Zeng, Temperature dependence of the mechanical properties and the inner structures of natural rubber reinforced by *in situ* polymerization of zinc dimethacrylate, J. Appl. Polym. Sci. 128 (2013) 2350–2357.
[66] P. Rublon, B. Huneau, N. Saintier, S. Beurrot, A. Leygue, E. Verron, D. Berghezan, *In situ* synchrotron wide-angle X-ray diffraction investigation of fatigue cracks in natural rubber, J. Synchrotron. Radiat. 20 (2013) 105–109.
[67] S. Beurrot-Borgarino, B. Huneau, E. Verron, P. Rublon, Strain-induced crystallization of carbon black-filled natural rubber during fatigue measured by in situ synchrotron X-ray diffraction, Int. J. Fatig. 47 (2013) 1–7.
[68] M.J. Brock, M.J. Hackathorn, The synergistic effect of natural rubber on the crystallization of lithium poly(isoprene)S (coral rubber), Rubber Chem. Technol. 45 (1972) 1303–1314.
[69] D.R. Burfield, Y. Tanaka, Cold crystallization of natural rubber and its synthetic analogues: the influence of chain microstructure, Polymer 28 (1987) 907–910.
[70] P. Corradini, Conformation of polymer molecules and entropy of melting, J. Polym. Sci. Polym. Symp. 50 (1975) 327–344.
[71] G. Allegra, M. Bruzzone, Effect of entropy of melting on strain-induced crystallization, Macromolecules 16 (1983) 1167–1170.
[72] S. Kawahara, T. Kakubo, N. Nishiyama, Y. Tanaka, Y. Isono, J.T. Sakdapipanich, Crystallization behavior and strength of natural rubber: skim rubber, deproteinized natural rubber, and pale crepe, J. Appl. Polym. Sci. 78 (2000) 1510.
[73] A.N. Gent, S. Kawahara, J. Zhao, Crystallization and strength of natural rubber and synthetic poly(isoprene-1,4-cis), Rubber Chem. Technol. 71 (1998) 668.
[74] T. Kakubo, A. Matsuura, S. Kawahara, Y. Tanaka, Origin of characteristic properties of natural rubber—effect of fatty acids on crystallization of poly(isoprene-1,4-cis), Rubber Chem. Technol. 71 (1998) 70–75.
[75] S. Kawahara, T. Kakubo, J.T. Sakdapipanich, Y. Isono, Y. Tanaka, Characterization of fatty acids linked to natural rubber—role of linked fatty acids on crystallization of the rubber, Polymer 41 (2000) 7483–7488.
[76] S. Kawahara, Y. Isono, T. Kakubo, Y. Tanaka, E. Aik-Hwee, Crystallization behavior and strength of natural rubber isolated from different HeveaClone, Rubber Chem. Technol. 73 (2000) 39.
[77] Y. Tanaka, Structural characterization of natural polyisoprenes: solve the mystery of natural rubber based on structural study, Rubber Chem. Technol. 74 (2001) 355.
[78] Y. Tanaka, L. Tarachiwin, Recent advances in structural characterization of natural rubber, Rubber Chem. Technol. 82 (2009) 283.
[79] O. Chaikumpollert, Y. Yamamoto, K. Suchiva, S. Kawahara, Protein-free natural rubber, Colloid Polym. Sci. 290 (2012) 331–338.
[80] S. Amnuaypornsri, S. Toki, B.S. Hsiao, J. Sakdapipanich, The effects of end-linking network and entanglement to stress–strain relation and strain-induced crystallization of un-vulcanized and vulcanized natural rubber, Polymer 53 (2012) 3325–3330.
[81] S. Toki, J. Che, L. Rong, B.S. Hsiao, S. Amnuaypornsri, A. Nimpaiboon, J. Sakdapipanich, Entanglements and networks to strain-induced crystallization and stress–strain relations in natural rubber and synthetic polyisoprene at various temperatures, Macromolecules 46 (2013) 5238–5248.
[82] P.H. Hermans, A. Weidinger, Textil. Res. J. 31 (1961) 558–571.
[83] R.J. Samuels, In: structured polymer properties, John Wiley & Sons, New York, 1971, p. 28.
[84] M. Kakudo, N. Kasai, In: X-ray diffraction by polymers, Elsevier, Amsterdam, 1972, p. 252.
[85] L.E. Alexander, in: In: X-ray diffraction methods in polymer science, Krieger RE, New York, 1979, p. 210.
[86] W.W. Schloman, D. McIntyre, A.S. Hilton, R.T. Beinor, J. Appl. Polym. Sci. 60 (1996) 1015–1023.
[87] W.W. Schloman Jr., F. Wyzgoski, D. McIntyre, K. Cornish, D.J. Siler, Rubber Chem. Technol. 69 (2006) 215–222.
[88] D.K. Stumpf, D.T. Ray, W.W. Schloman, J. Am. Oil. Chem. Soc. 78 (2001) 217–218.
[89] K. Cornish, J.L. Williams, M. Kirk, V.H. Teetor, D.T. Ray, Ind. Biotechnol. 5 (2009) 245–252.
[90] A. Estilai, Rubber Chem. Technol. 60 (1987) 245–251.
[91] Angulo-Sanchez, Proceedings Third International Guayule Conf., 1983.
[92] J. West, E. Rodriguez, Rubber Chem. Technol. 60 (1987) 888–892.
[93] M.W. Duch, D.M. Grant, Macromolecules 3 (1970) 165–174.
[94] T. Schmidt, M. Lenders, A. Hillebrand, N. van Deenen, O. Munt, R. Reichelt, C.S. Gronover, BMC Biochem. 11 (2010) 11.
[95] FDA medical alert: *allergic reactions to latex-containing medical devices*, 1991. Rockville.
[96] T. Karino, Y. Ikeda, Y. Yasuda, S. Kohjiya, M. Shibayama, Biomacromolecules 8 (2007) 693–699.
[97] A. D'Amato, A. Bachi, E. Fasoli, E. Boschetti, G. Peltre, H. Sénéchal, P.G. Righetti, J. Proteom. 73 (2010) 1368–1380.
[98] W.W. Schloman Jr., R.A. Hively, A. Krishen, A.M. Andrews, J. Agric. Food Chem. 31 (1983) 873–876.
[99] R.W. Scora, J. Kumamoto, J. Agric. Food Chem. 27 (1979) 642–643.
[100] S.C. Nyburg, A statistical structure for crystalline rubber, Acta Crystallogr. 7 (1954) 385.
[101] G. Natta, P. Corradini, Über die Kristallstrukturen des 1,4-cis-Polybutadiens und des 1,4-cis-Polyisoprens, Angew. Chem. 68 (1956) 615–616.
[102] A. Immirzi, C. Tedesco, G. Monaco, A. Tonelli, E., Crystal structure and melting entropy of natural rubber, Macromolecules 38 (2005) 1223.
[103] G. Rajkumar, J.M. Squire, S. Arnott, A new structure for crystalline natural rubber, Macromolecules 39 (2006) 7004.
[104] J. Che, C. Burger, S. Toki, L. Rong, B.S. Hsiao, S. Amnuaypornsri, J. Sakdapipanich, Crystal and crystallites structure of natural rubber and synthetic poly(isoprene-1,4-cis) by a new two dimensional wide angle X-ray diffraction simulation method. I. Strain-induced crystallization, Macromolecules 46 (2013) 4520–4528.
[105] C. De Rosa, F. Auriemma, Crystals and crystallinity in polymers: diffraction analysis of ordered and disordered crystals, John Wiley & Sons, Inc., Hoboken, New Jersey, 2014, pp. 202–204 [Chapter 4.2.3].
[106] H.G. Kim, L. Mandelkem, Multiple melting transitions in natural rubber, J. Polym. Sci. A-2 10 (1972) 1125–1133.
[107] E.N. Dalal, K.D. Taylor, P.J. Phillips, The equilibrium melting temperature of cis-polyisoprene, Polymer 24 (1983) 1623.
[108] D.E. Roberts, L. Mandelkern, The melting temperature of natural rubber networks, J. Am. Chem. Soc. 82 (1960) 1091–1095.
[109] E.N. Dalal, P.J. Phillips, Pressure dependence of the equilibrium melting temperature and fold surface free energy of cis-polyisoprene, Macromolecules 16 (1983) 1754–1760.
[110] A.N. Gent, S. Kawahara, J. Zhao, Crystallization and strength of natural rubber and synthetic *poly(isoprene-1,4-cis)*, Rubber Chem. Technol. 71 (1998) 668.
[111] A.N. Gent, Trans. Faraday Soc. 50 (1954) 521–533.
[112] O. Chaikumpollert, Y. Yamamoto, K. Suchiva, P.T. Nghia, S. Kawahara, Polym. Adv. Technol. 23 (2012) 825–882.
[113] G. Russo, L. Parravicini, F. Auriemma, V. Petraccone, G. Guerra, R. Bianchi, G. Di Dino, V.M. Vitagliano, J. Polym. Sci. (1997) 889–896.